TECHNICAL ARTICLE

Vibrations of L-Shaped Beam Structures With a Crack: Analytical Approach and Experimental Validation

C.A. Rossit[1,2], D.V. Bambill[1,2], A.R. Ratazzi[1], and S. Maiz[1]

1 Departamento de Ingeniería, Instituto de Mecánica Aplicada (IMA), Universidad Nacional del Sur (UNS), Bahía Blanca, Argentina
2 Consejo Nacional de Investigaciones Científicas y Técnicas (CONICET), Bahía Blanca, Argentina

Keywords
L-Shaped Beam, L-Beam, Crack, Vibrations, Elastic Hinge, Damage

Correspondence
C.A. Rossit
Departamento de Ingeniería, Instituto de Mecánica Aplicada (IMA)
Universidad Nacional del Sur (UNS)
8000 Bahía Blanca
Buenos Aires
Argentina
Email: carossit@criba.edu.ar

Received: March 17, 2014;
accepted: December 22, 2014

doi:10.1007/s40799-016-0104-y

Abstract

A crack on a structural member introduces a local flexibility which is function of the crack depth. This new flexibility condition changes the dynamic behavior of the structure. The knowledge of the influence of the crack on the characteristic dynamic parameters makes it possible to determine both the crack position and its magnitude. A large number of research papers have been written on the subject, most of them on straight beams of a single segment. However, despite the importance of L-shaped beams in a variety of technological applications, very limited information is available for the case of such structures. In this article, a cracked L-beam structure is studied by an analytical approach which is validated by experimental measurements. The Euler–Bernoulli beam theory is assumed to describe the transversal displacements and the crack is modeled by means of an elastically restrained hinge. A special device was designed to measure experimentally the natural frequencies of steel L-beams structures. The natural frequencies of in plane vibrations of L-beam structures are obtained considering a crack at different positions as well as of different depths. Values obtained with the analytical solution are satisfactorily compared with experimentally measured frequencies and the values reported in previous studies on the subject published by other authors.

Introduction

The problem of the influence of a crack in a welded joint on the dynamic behavior of a structural member has been studied in a thorough paper by Chondros and Dimarogonas.[1]

The static and dynamic analysis of beams with single or multiple concentrated damages, produced by cracks, has received an increasing interest in recent years.

A very complete description of the state of the art in the field with the mention and description of the most important work was done by Caddemi and Morassi,[2] whose reading is recommended.

There it is explained that generally, it is assumed that the amplitude of the deformation is enough to maintain the crack always open, this model offers the great advantage to be linear and, therefore, it leads to efficient formulations for solving both static and dynamic problems.

From earliest studies, it is clear that localized damage produces a local reduction in the stiffness of the beam.[3] Many models have been proposed in the literature to describe open cracks on beams, the flexibility modeling of cracks is quite common.[4] In the case of beams under plane flexural deformation, a crack is modeled by inserting a massless rotational elastic spring at the damaged cross section.[5,6]

Many researchers have studied the topic of equivalent flexibility of the spring which models the crack.[7–15] Among them, it can be mentioned that the expression of Chondros et al.[15] is the most widely used.

Most of the papers deal with straight beams of a single stretch. Far less are related with frames.[16–18]

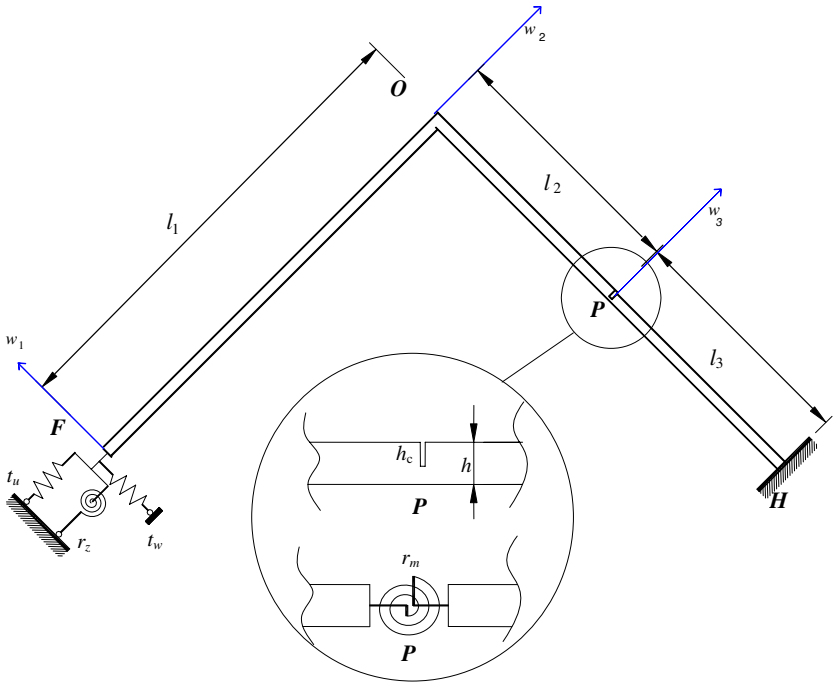

Figure 1 L-frame structure.

The use of the L-shaped structures is widespread in many fields of engineering, including modern applications in robotics.[19]

In present work, an L-shaped beam with a crack in one of the sections is studied. In order to perform this study, it is important to have an analytical procedure which allows determining the dynamic parameters of cracked L-beams structures. And it is known that an essential condition to ensure the reliability of an analytical procedure is the experimental verification of its accuracy, especially in a case like this in which the values available in the literature are scarce.

The objective of this study is twofold: The proposition of a classical elastic model where the crack is modeled by a rotational spring calculated following Chondros' theory and shows the excellent concordance that the proposed model exhibits with experimental measurements performed on a device specially designed.

In addition, information is provided about the variation of the natural frequencies of an L-beam produced by a crack at different positions and of different depths and the usefulness of the combination of the posed analytical approach and experimental measures in crack detection is demonstrated.

Structural Model and Analytical Solution

The study deals with the vibration of L-shaped beams assuming an internal crack in different positions in one of the beams of the system.

The two parts of the L-shaped structure are joined at right angle, with the end of one of them clamped and the end of the other elastically restrained. Figure 1 depicts the structure under study.

The position of the crack is defined by the coordinate l_2 and locally affects the flexural stiffness of the L-beam. It is modeled as a massless, rotational elastic spring at the damaged cross section connecting the two adjacent segments of the beam.

The magnitude adopted for the flexibility constant of the equivalent spring (β_C), is obtained by means of the expression proposed by Chondros et al.[15] which was found with fracture mechanics methods:

$$\beta_C = \frac{6\pi\left(1-\nu^2\right)h}{EI}\phi_C(z) \tag{1}$$

with

$$\phi_c(z) = 0.6272\,z^2 - 1.04533\,z^3 + 4.5948\,z^4 - 9.973\,z^5 + 20.2948\,z^6 - 33.0351\,z^7 + 47.1063\,z^8 - 40.7556\,z^9 + 19.6\,z^{10}$$

and $z = {}^{h_C}/_{h}$, while h is the height of the cross section and h_C is the depth of the crack.

Three beam members are defined in the structure: the beam FO of length l_1, the beam OP of length l_2 and the beam PH of length l_3; each of them having uniform properties. The beams are modeled using the Euler–Bernoulli beam theory.

The external end H is a classical clamped support and the external end F is supported by two

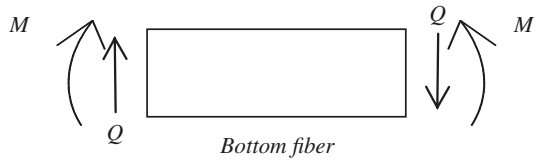

Figure 2 Sign convention for positive shear force (*Q*) and bending moment (*M*).

translational springs of stiffness t_w and t_u and a rotational spring of stiffness r_z. At section *P*, there is the crack. To model the crack, it is supposed an internal hinge elastically restrained against rotation between beams 2, *OP*, and 3, *PH*, this semirigid connection is materialized by a rotational spring of stiffness:

$$r_m = {}^{1}/_{\beta_C}. \tag{2}$$

The flexural rigidity, the mass density, the length, and the area of the cross section of each beam are E_iI_i, ρ_i, l_i, and A_i, with $i = 1, 2, 3$.

Three coordinate systems are located as they are shown in Fig. 1, and its origins are taken to be at points *F*, *O*, and *P* in each beam. At abscissa x_i ($0 \le x_i \le l_i$), w_i is the transverse displacement of the beam *i*, and $\theta_i = \partial w_i/\partial x_i$ is the section rotation at any time *t*. The deformation of a beam in *x* direction is not taken into account, because the beams are considered infinitely rigid in the axial direction.

The sign convention used for the positive shear force spins an element clockwise (up on the left and down on the right). Likewise the normal convention for a positive bending moment elongates the bottom fiber of the beam. Figure 2 shows the sign convention to be employed.

For free vibration, the bending moment and the shear force expressions are:

$$M_i(x_i, t) = E_iI_i\frac{\partial^2 w_i(x_i, t)}{\partial x_i^2};\ Q_i(x_i, t) = E_iI_i\frac{\partial^3 w_i(x_i, t)}{\partial x_i^3} \tag{3}$$

To express equations in dimensionless form, the nondimensional parameter is introduced:

$$X_i = {}^{x_i}/_{l_i};\ \text{with}\ X_i \in [0, 1]\quad \forall i\ = 1, 2, 3 \tag{4}$$

The displacements w_i, and θ_i may be expressed in terms of the dimensionless coordinates as follows:

$$W_i(X_i, t) = \frac{w_i(x_i, t)}{l_i};\quad \theta_i(X_i, t) = \frac{\partial W_i(X_i, t)}{\partial X_i} = \frac{\partial w_i(x_i, t)}{\partial x_i} \tag{5}$$

The characteristics of beam 1 are used as ''reference'':

$$EI = E_1I_1,\ \rho A = \rho_1A_1,\ l = l_1 \tag{6}$$

to define the ratios:

$$\nu_{EI_i} = \frac{E_iI_i}{EI},\ \nu_{\rho A_i} = \frac{\rho_iA_i}{\rho A},\ \nu_{l_i} = \frac{l_i}{l} \tag{7}$$

the dimensionless spring stiffness:

$$T_w = t_w\frac{l^3}{EI},\ T_u = t_u\frac{l^3}{EI},\ R_z = r_z\frac{l}{EI},\ R_m = r_m\frac{l}{EI} \tag{8}$$

Under the described conditions and applying the technique of variational calculus,[20] the governing differential equations of the problem and the boundary and continuity conditions are:

$$\frac{\partial^4 W_1}{\partial X_1^4}(X_1, t) + k_1^4\frac{\partial^2 W_1}{\partial t^2}(X_1, t) = 0 \tag{9}$$

$$\frac{\partial^4 W_2}{\partial X_2^4}(X_2, t) + k_2^4\frac{\partial^2 W_2}{\partial t^2}(X_2, t) = 0 \tag{10}$$

$$\frac{\partial^4 W_3}{\partial X_3^4}(X_3, t) + k_3^4\frac{\partial^2 W_3}{\partial t^2}(X_3, t) = 0 \tag{11}$$

with $k_i^4 = \frac{\rho_iA_i}{E_iI_i}l_i^4$, $i = 1, 2, 3$.

$$\frac{\nu_{EI_1}}{\left(\nu_{l_1}\right)^2}\frac{\partial^3 W_1}{\partial X_1^3}(0, t) + T_w\nu_{l_1}W_1(0, t) = 0 \tag{12}$$

$$\frac{\nu_{EI_1}}{\nu_{l_1}}\frac{\partial^2 W_1}{\partial X_1^2}(0, t) - R_z\left(\frac{\partial W_1}{\partial X_1}(0, t)\right) = 0 \tag{13}$$

$$\frac{\nu_{EI_2}}{\left(\nu_{l_2}\right)^2}\frac{\partial^3 W_2}{\partial X_2^3}(0, t) + T_u\nu_{l_2}W_2(0, t) - k_1^4\nu_{l_1}\nu_{l_2}\frac{\partial^2 W_2}{\partial t^2}(0, t) = 0 \tag{14}$$

$$\nu_{l_1}W_1(1, t) = 0 \tag{15}$$

$$\frac{\partial W_1}{\partial X_1}(1, t) = \frac{\partial W_2}{\partial X_2}(0, t) \tag{16}$$

$$\frac{\nu_{EI_1}}{\nu_{l_1}}\frac{\partial^2 W_1}{\partial X_1^2}(1, t) = \frac{\nu_{EI_2}}{\nu_{l_2}}\frac{\partial^2 W_2}{\partial X_2^2}(0, t) \tag{17}$$

$$\nu_{l_2}W_2(1, t) = \nu_{l_3}W_3(0, t) \tag{18}$$

$$\frac{\nu_{EI_2}}{\nu_{l_2}^2}\frac{\partial^3 W_2}{\partial X_2^3}(1, t) - \frac{\nu_{EI_3}}{\nu_{l_3}^2}\frac{\partial^3 W_3}{\partial X_3^3}(0, t) = 0 \tag{19}$$

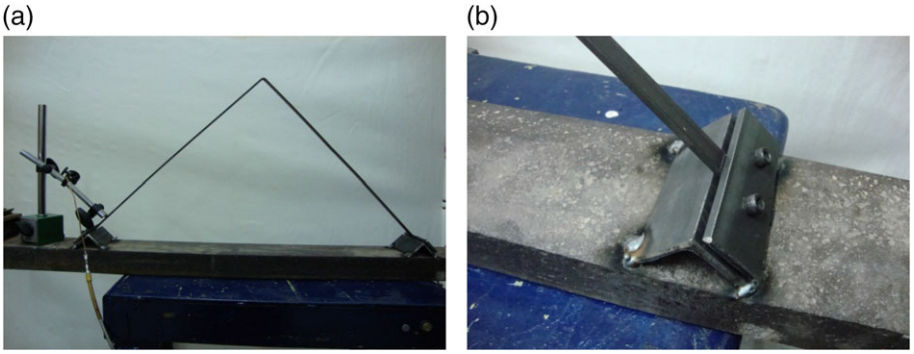

Figure 3 (a) and (b) Experimental device: clamped-lamped L-beam.

$$\frac{v_{EI_2}}{v_{l_2}}\frac{\partial^2 W_2}{\partial X_2^2}(1,t) - R_m\left(\frac{\partial W_3(0,t)}{\partial X_3} - \frac{\partial W_2(1,t)}{\partial X_2}\right) = 0 \quad (20)$$

$$\frac{v_{EI_3}}{v_{l_3}}\frac{\partial^2 W_3}{\partial X_3^2}(0,t) - R_m\left(\frac{\partial W_3(0,t)}{\partial X_3} - \frac{\partial W_2(1,t)}{\partial X_2}\right) = 0 \quad (21)$$

$$v_{l_3} W_3(1,t) = 0 \quad (22)$$

$$\frac{\partial W_3}{\partial X_3}(1,t) = 0 \quad (23)$$

The last term in Eq. 14 is due to the rigid body axial translation of beam 1 of length l_1, which is a consequence of assuming infinity axial rigidity.

Using the well-known separation of variables method to solve Eqs. 9 to 11, free vibrations of the system can be expressed in the form:

$$W_1(X_1,t) = \sum_{n=1}^{\infty} W_{1n}(X_1)\ e^{i\omega t} \quad (24)$$

$$W_2(X_2,t) = \sum_{n=1}^{\infty} W_{2n}(X_2)\ e^{i\omega t} \quad (25)$$

$$W_3(X_3,t) = \sum_{n=1}^{\infty} W_{3n}(X_3)\ e^{i\omega t} \quad (26)$$

The functions W_{1n}, $W_{2n,}$ and W_{3n} represent the corresponding transverse modes of natural vibration of each beam member and are given by:

$$W_{1n}(X_1) = C_1\cosh(\lambda_n\alpha_1 X_1) + C_2\mathrm{sen}h(\lambda_n\alpha_1 X_1) + C_3\cos(\lambda_n\alpha_1 X_1) + C_4\mathrm{sen}(\lambda_n\alpha_1 X_1) \quad (27)$$

$$W_{2n}(X_2) = C_5\cosh(\lambda_n\alpha_2 X_2) + C_6\mathrm{sen}h(\lambda_n\alpha_2 X_2) + C_7\cos(\lambda_n\alpha_2 X_2) + C_8\mathrm{sen}(\lambda_n\alpha_2 X_2) \quad (28)$$

$$W_{3n}(X_3) = C_9\cosh(\lambda_n\alpha_3 X_3) + C_{10}\mathrm{sen}h(\lambda_n\alpha_3 X_3) + C_{11}\cos(\lambda_n\alpha_3 X_3) + C_{12}\mathrm{sen}(\lambda_n\alpha_3 X_3) \quad (29)$$

where $\alpha_i = v_{l_i}\ \sqrt[4]{v_{\rho A_i}/v_{EI_i}}$ is a mechanical and geometrical parameter, with $i = 1, 2, 3$; $\lambda_n = \sqrt[4]{l^4\omega_n^2\,\rho A/EI}$ is the dimensionless frequency coefficient of mode of vibration n and $C_1, C_2, \ldots, C_{12}$ are arbitrary constants to be determined.

Replacing Eqs. 27, 28, and 29 in Eqs. 24, 25, and 26; and these ones in Eqs. 12 to 23, a linear system of equations in the unknown constants $C_1, C_2, \ldots, C_{12}$ is obtained.

For a nontrivial solution to exist, the determinant of the coefficient matrix in the linear system of equations should be equal to zero and the roots of the transcendental frequency equation are the dimensionless frequency coefficients λ_n of the mechanical system in Fig. 1.

The results were determined by using the Mathematica software[21] with six significant figures.

Experimental Device

Two particular cases were modeled, a free-clamped (F-C) and a clamped–clamped (C-C) L-beam.

A bar of steel 5/8 '' × 1/8'' ($b = 15.875$ mm, $h = 3.175$ mm) was employed.

Both members the same length ($l_1 = l_2 + l_3$), cross-sectional area, and material properties:

$$v_{\rho A_i} = 1; \quad v_{EI_i} = 1; \quad \forall \quad i = 1, 2, 3;$$
$$v_{l_1} = 2v_{l_2} = 2v_{l_3} = 1$$

The length of each member was 420 mm for the F-C case and 446 mm for the C-C.

Figure 3(a) and (b) shows the clamped–clamped model tested.

The crack was modeled with a thickness of 1 mm. All precautions were taken so that the cut is made smoothly and its depth be uniform: A piece of hard steel was employed, with a gap where the beam is embedded up to the desired depth (Fig. 4(a) and (b)).

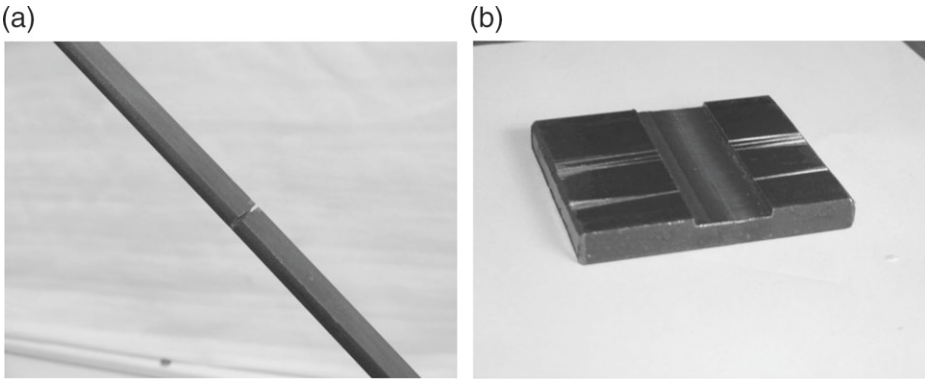

Figure 4 (a) and (b) Crack produced in the strip.

The beam was excited with an impact hammer near the clamped end, where there are no nodes of the modal shapes of the first five frequencies.

In order not to disturb the behavior of the structure, measurements were taken with a proximitor. A Provibtech device, TMO 180, was employed. The displacement signal was read and processed with a two channel vibration analyzer Vibxpert II, with 24 bits of resolution and 1000 Hz of sample frequency.

To evaluate the measured values, it is needed to know the Young modulus E and the density ρ of the employed material.

Because these two parameters, in dynamical applications, are always involved by means of the ratio $\sqrt{\frac{E}{\rho}}$, the following procedure was followed:

A value widely verified in solid mechanics was taken as reference: the fundamental frequency of a cantilever beam. It is known that the corresponding eigenvalue is 1.8751.[22]

A cantilever beam of length 417 mm was built with the same strap of the L-beam.

The measured frequency: 14.85 Hz, then:

$$f = \frac{1}{2\pi}\frac{\lambda^2}{l^2}\sqrt{\frac{EI}{\rho A}}, 14.85\text{Hz} = \frac{1}{2\pi}\frac{(1.8751)^2}{(0.417\text{m})^2}\sqrt{\frac{Eh^2}{\rho\ 12}}$$

$$\Rightarrow \sqrt{\frac{E}{\rho}} = 5034.7\frac{m}{\text{seg}}$$

This value, which is the speed of a longitudinal wave in steel, is employed in the numerical determinations.

Numerical Results

In order to verify the accuracy of the procedure, two particular cases of the proposed analytical approach are modeled:

Free-clamped L-beam, without internal hinge: $T_u = T_w = R_z = 0$; $R_m \to \infty$;

Clamped–clamped L-beam, without internal hinge: $T_u = T_w = R_z = R_m \to \infty$.

Table 1 presents the first five natural frequencies of vibration. The values obtained by means of the analytical approach are in very good agreement with results available in the literature.

Experimental determinations are also performed and data show a striking agreement with aforementioned values.

Tables 2–6 compare the results between experimental measurements in a device with a crack artificially produced and the proposed analytical procedure with a crack modeled following Chondros' criterion. A free-clamped L-beam with $l_1 = l_2 + l_3$ is considered, different locations (l_2/l_1) and depths (h_c/h) of the crack are taken into account. Applying Eqs. 1, 2, and 8, one obtains R_m for each particular situation.

As it can be seen, the experimental values are again in excellent agreement, from an engineering viewpoint, with those obtained by means of the analytical procedure. There are just five situations where differences are upon 5%, but in no case exceed than 10%.

Figure 5 shows the effect of the depth of a crack at different locations on the natural frequencies.

The magnitudes of frequencies in the damaged structure f are related to the frequency of the structure without crack which is named f_0.

In general, the frequencies decrease as the depth of the crack increases

As it can be observed, the second frequency is not affected by the crack when occurs in the middle of the second member. It can be deduced that the corresponding modal shape of the undamaged structure has no curvature at that point.

Figure 6 shows the effect that the position of a crack ($h_c/h = 0.75$) causes in the first three natural frequencies of the free-clamped L-beam structure. Again, it is observed that the second frequency does

Table 1 First five natural frequencies for F-C and C-C L-beams

Free-clamped L-shaped beam						
i	1	2	3	4	5	
λ_i	1.0880	1.7869	3.9685	4.8021	7.0915	Lin and Ro[23] (eigenvalue)
λ_i	1.0821	1.7863	3.9684	4.8037	7.0982	Analytical (eigenvalue)
(f_i)	4.85	13.22	65.25	95.62	208.79	Analytical (Hz)
(f_i)	4.77	13.04	65.14	95.16	207.74	Experimental (Hz)
Clamped–clamped L-shaped beam						
i	1	2	3	4	5	
λ_i	3.9222	4.7145	7.0376	7.7588	10.007	Albarracín et al.[24] (eigenvalue)
λ_i	3.9331	4.7235	7.0540	7.8255	10.149	Analytical (eigenvalue)
(f_i)	56.62	82.08	183.07	225.29	378.99	Analytical (Hz)
(f_i)	56.76	83.01	182.50	228.88	382.08	Experimental (Hz)

Table 2 First five natural frequencies for F-C L-beams with a crack in the sixth of the second member

l_2/l_1	h_c/h	R_m		1	2	3	4	5	
1/6	0.25	220	λ_i	1.0812	1.7862	3.9680	4.8015	7.0935	Analytical (eigenvalue)
			(f_i)	4.84	13.22	65.24	95.53	208.15	Analytical (Hz)
			(f_i)	4.77	13.04	65.14	95.10	207.58	Experimental (Hz)
	0.50	41	λ_i	1.0800	1.7769	3.9619	4.8020	7.0660	Analytical (eigenvalue)
			(f_i)	4.83	13.08	65.04	95.55	206.90	Analytical (Hz)
			(f_i)	4.66	12.93	65.02	95.09	207.42	Experimental (Hz)
	0.75	7.9	λ_i	1.0698	1.7416	3.9356	4.7905	6.9521	Analytical (eigenvalue)
			(f_i)	4.74	12.57	64.18	95.10	200.28	Analytical (Hz)
			(f_i)	4.34	12.60	64.58	95.10	207.48	Experimental (Hz)

Table 3 First five natural frequencies for F-C L-beams with a crack in the third of the second member

l_2/l_1	h_c/h	R_m		1	2	3	4	5	
1/3	0.25	220	λ_i	1.0810	1.7857	3.9661	4.8035	7.0947	Analytical (eigenvalue)
			(f_i)	4.84	13.21	65.18	95.61	208.58	Analytical (Hz)
			(f_i)	4.77	13.04	65.14	95.05	207.14	Experimental (Hz)
	0.50	41	λ_i	1.078	1.7831	3.9529	4.7961	7.0783	Analytical (eigenvalue)
			(f_i)	4.82	13.17	64.75	95.32	207.62	Analytical (Hz)
			(f_i)	4.66	12.98	64.92	94.45	204.22	Experimental (Hz)
	0.75	7.9	λ_i	1.0633	1.7709	3.8920	4.7657	6.999	Analytical (eigenvalue)
			(f_i)	4.68	13.00	62.77	94.12	203.04	Analytical (Hz)
			(f_i)	4.38	12.93	64.15	93.47	196.32	Experimental (Hz)

Table 4 First five natural frequencies for F-C L-beams with a crack in the middle of the second member

l_2/l_1	h_c/h	R_m		1	2	3	4	5	
1/2	0.25	220	λ_i	1.0814	1.7862	3.9666	4.8003	7.0977	Analytical (eigenvalue)
			(f_i)	4.85	13.22	65.20	95.49	208.76	Analytical (Hz)
			(f_i)	4.71	13.01	64.98	94.83	207.63	Experimental (Hz)
	0.50	41	λ_i	1.0770	1.7861	3.9558	4.7801	7.0942	Analytical (eigenvalue)
			(f_i)	4.81	13.22	64.84	94.68	208.56	Analytical (Hz)
			(f_i)	4.66	12.99	64.50	93.89	207.46	Experimental (Hz)
	0.75	7.9	λ_i	1.0550	1.7856	3.9026	4.700	7.080	Analytical (eigenvalue)
			(f_i)	4.61	13.21	63.11	91.50	207.72	Analytical (Hz)
			(f_i)	4.33	12.99	60.98	89.97	206.79	Experimental (Hz)

Table 5 First five natural frequencies for F-C L-beams with a crack in the second third of the second member

l_2/l_1	h_c/h	R_m		1	2	3	4	5	
2/3	0.25	220	λ_i	1.0810	1.7860	3.9684	4.8033	7.0924	Analytical (eigenvalue)
			(f_i)	4.84	13.22	65.25	95.61	208.45	Analytical (Hz)
			(f_i)	4.77	13.04	65.03	95.10	207.41	Experimental (Hz)
	0.50	41	λ_i	1.0750	1.7850	3.9671	4.7950	7.0661	Analytical (eigenvalue)
			(f_i)	4.79	13.20	65.22	95.28	206.91	Analytical (Hz)
			(f_i)	4.77	12.98	64.48	94.94	205.80	Experimental (Hz)
	0.75	7.9	λ_i	1.0450	1.7803	3.9593	4.7578	6.9434	Analytical (eigenvalue)
			(f_i)	4.53	13.13	64.96	93.81	199.78	Analytical (Hz)
			(f_i)	4.49	12.43	59.70	94.16	192.59	Experimental (Hz)

Table 6 First five natural frequencies for F-C L-beams with a crack in the fifth sixth of the second member

l_2/l_1	h_c/h	R_m		1	2	3	4	5	
5/6	0.25	220	λ_i	1.0800	1.7849	3.9684	4.8047	7.0982	Analytical (eigenvalue)
			(f_i)	4.84	13.20	65.26	95.66	208.79	Analytical (Hz)
			(f_i)	4.77	13.04	65.14	95.16	207.36	Experimental (Hz)
	0.50	41	λ_i	1.0720	1.7791	3.9652	4.8021	7.0975	Analytical (eigenvalue)
			(f_i)	4.76	13.12	65.15	95.56	208.75	Analytical (Hz)
			(f_i)	4.77	12.88	64.97	95.05	205.79	Experimental (Hz)
	0.75	7.9	λ_i	1.0330	1.7557	3.9523	4.7919	7.0939	Analytical (eigenvalue)
			(f_i)	4.43	13.77	64.73	95.15	208.54	Analytical (Hz)
			(f_i)	4.66	12.16	63.15	94.11	196.37	Experimental (Hz)

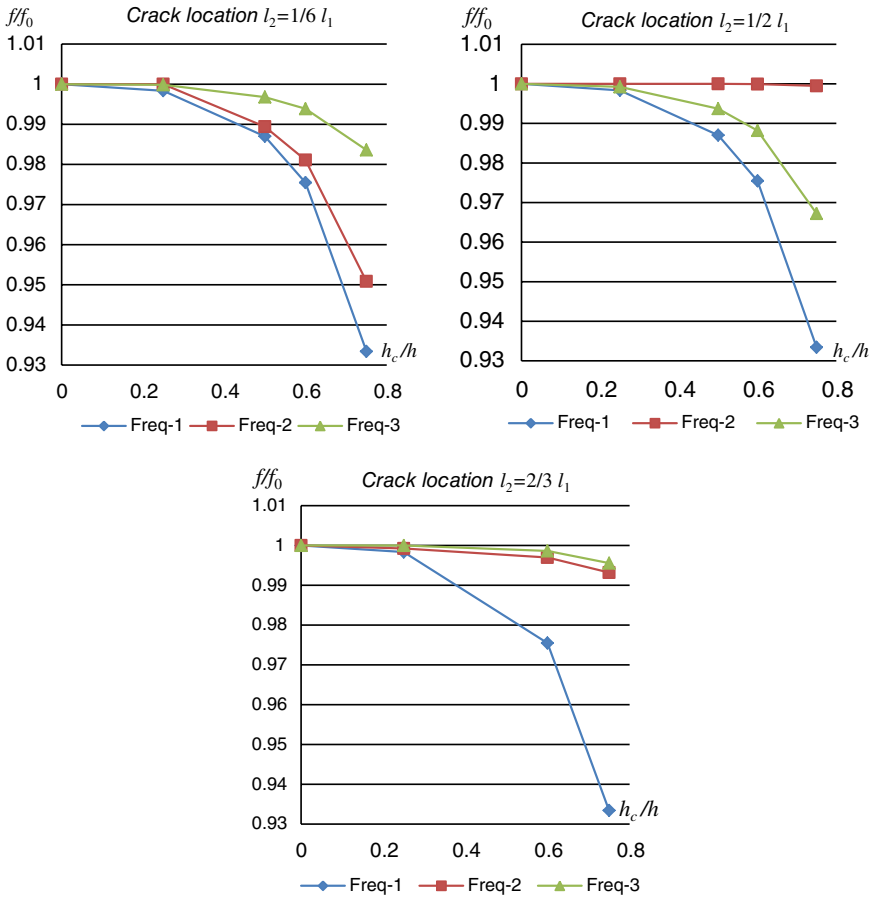

Figure 5 Relative decrease of the first three natural frequencies with the depth of a crack located at different positions of the second member of a free-clamped L-beam.

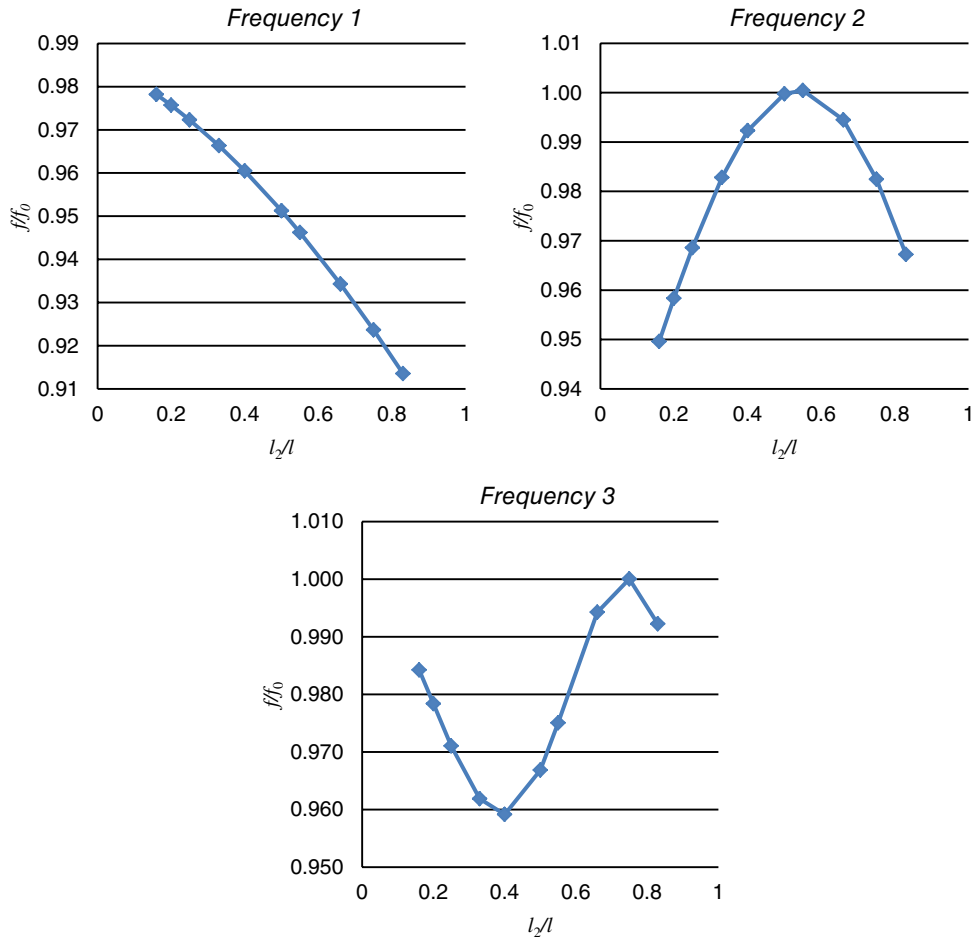

Figure 6 Influence of the location in the second member of a crack ($h_c/h = 0.75$) on the relative decrease of the first three natural frequencies in a free-clamped L-beam.

not vary when the crack is in the middle of the segment.

Then, we use the available information in order to demonstrate the usefulness of the proposed analytical model in crack detection.

The inverse method, widely used in the scientific literature (Rosales et al.[25], Labib et al.[26]), is employed to predict position (l_2) and depth (h_c/h) of a crack from measured values of frequency in the damaged structure.

As is known (Owolabi et al.[27]), measuring the first three natural frequencies (f_n, with $n = 1, 2, 3$) will be enough to determine the crack location and depth for a beam-like structure with a single crack. Each of the first three dimensionless values: $\lambda_n = \sqrt[4]{l^4 (2\pi f_n)^2 \, \rho A/EI}$ of every measured frequency is introduced into the frequency transcendental equation formed with the system of Eqs. 13 to 22. Plotting in a curve, the results of the frequency transcendental equation for a particular mode n is obtained a contour line (Rm versus l_2). Each point of the curve represents a combination of different crack locations l_2 and crack depths (identified by R_m), that according to the analytical model, correspond to the measured frequency.

Three contour curves are obtained for the first, second, and third modes. Overlaying those three graphs, it is possible to obtain an intersection point. The cross point has particular coordinates: l_2 and R_m. The position of the crack is represented by l_2 and R_m represents the crack depth according to Eqs. 1, 2, and 8.

The situation, identified with: $l_2/l_1 = 1/2$, $h_c/h = 0.25$, $f_1 = 4.71$ Hz, $f_2 = 13.01$ Hz, $f_3 = 64.98$ Hz (Table 4), is used to illustrate the procedure.

Figure 7 shows three curves which are contour lines, according to the analytical model, of each measured frequency, ($n = 1$, 2, and 3). They do not intersect exactly at a point, but they describe a small

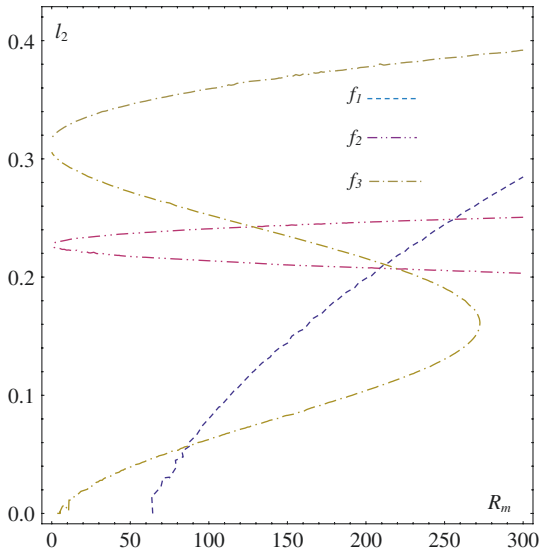

Figure 7 Set of values R_m, l_2 corresponding to every measured frequency in a damaged free-clamped L-beam.

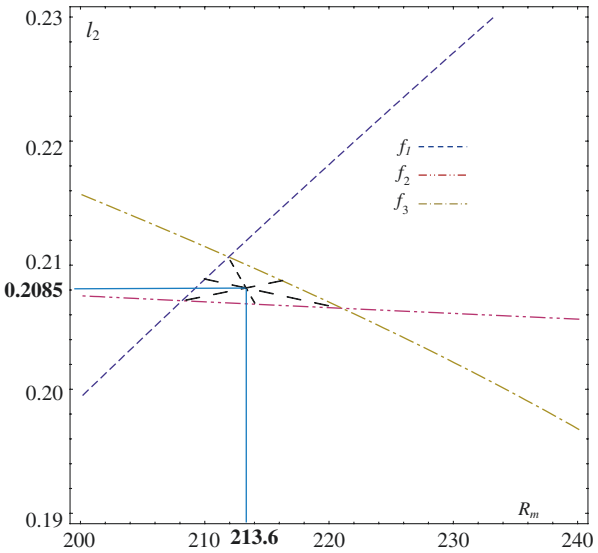

Figure 8 Enlarged view of the area of intersection of curves.

triangular zone, that allows to estimate the position of the crack l_2 and the crack depth R_m.

There are different procedures for estimating the crack position and its depth (l_2, R_m). In the present analysis, the triangle enclosed by the points of intersection of each pair of curves (Fig. 8) is analyzed and its centroid is determined, it is the sought point: $l_2 = 208.5$ mm ($l_2/l_1 = 0.496$), $R_m = 213.6$ ($h_c/h = 0.254$).

Those estimated values are in excellent agreement with the real position of the crack and its depth, an error of 0.36% of the length of the whole beam OH in the position and 0.4% of the section height in the crack depth.

The analytical approach was also verified, for some cases of the cracked clamped–clamped L-beam structure, comparing with experimental measurements.

Tables 7–9 show the obtained values by both paths.

As it can be seen, the experimental values are again in surprising agreement with those obtained by means of the analytical procedure. There is no case where the difference exceeds than 5%, and generally it is less than 2%

Conclusions

The convergence between the experimental and analytical values showed that a classical elastic model of the L-beam behavior in combination with the

Table 7 First five natural frequencies for C-C L-beams with a crack in the third of the second member

l_2/l_1	h_c/h	R_m		1	2	3	4	5	
1/3	0.50	44	λ_i	3.9195	4.7144	7.0155	7.7862	10.1331	Analytical (eigenvalue)
			(f_i)	56.45	81.67	180.86	217.40	377.32	Analytical (Hz)
			(f_i)	56.45	83.01	181.88	225.22	382.26	Experimental (Hz)
	0.75	8.4	λ_i	3.9117	4.6886	6.9269	7.7234	10.093	Analytical (eigenvalue)
			(f_i)	56.22	80.78	174.25	217.64	374.35	Analytical (Hz)
			(f_i)	56.15	80.57	167.24	217.9	377.81	Experimental (Hz)

Table 8 First five natural frequencies for C-C L-beams with a crack ($h_c/h = 0.75$) in the middle of the second member

l_2/l_1	h_c/h	R_m		1	2	3	4	5	
1/2	0.75	8.4	λ_i	3.8482	4.6617	7.03645	7.8254	9.9059	Analytical (eigenvalue)
			(f_i)	54.41	79.18	181.44	224.73	360.59	Analytical (Hz)
			(f_i)	52.49	78.13	183.72	227.05	348.51	Experimental (Hz)

Table 9 First five natural frequencies for C-C L-beams with a crack ($h_c/h = 0.75$) in the second third of the second member

l_2/l_1	h_c/h	R_m		1	2	3	4	5	
2/3	0.75	8.4	λ_i	3.8420	4.7007	6.9814	7.7194	10.136	Analytical (eigenvalue)
			(f_i)	54.02	80.86	177.82	217.27	376.77	Analytical (Hz)
			(f_i)	52.49	81.18	173.95	217.29	380.86	Experimental (Hz)

Chondros' representation of a crack constitutes a simple and reliable tool that allows to attack in a straightforward way the problem of an L-shaped structure with a crack. Its usefulness in crack detection is demonstrated.

The approach can be easily adapted to study all possible outer boundary conditions of the L-beam structure taking into account elastic constraints at both ends. Further cracks may be incorporated by including additional internal elastic hinges.

It is interesting to note the importance of carrying out experimental procedures as they are a sure way to verify analytical approaches.

Acknowledgments

The present work has been sponsored by Secretaría General de Ciencia y Tecnología of Universidad Nacional del Sur at the Department of Engineering, Consejo Nacional de Investigaciones Científicas y Técnicas (CONICET) and by Comisión de Investigaciones Científicas (CIC, Buenos Aires Province). The authors are grateful to Mr. Gabriel Leguizamón for his careful preparation of the experimental device. The authors are indebted to the reviewers for their thoughtful suggestions that helped to improve this work.

REFERENCES

1. Chondros, T.G., and Dimarogonas, A.D., ''Identification of Crack in Welded Joints of Complex Structure,'' *Journal of Sound and Vibration* **69**: 531–538 (1980).
2. Caddemi, S., and Morassi, A., ''Multi-Cracked Euler–Bernoulli Beams: Mathematical Modeling and Exact Solutions,'' *International Journal of Solids and Structures* **50**: 944–956 (2013).
3. Thomson, W.J., ''Vibration of Slender Bars with Discontinuities in Stiffness,'' *Journal of Applied Mechanics* **17**: 203–207 (1943).
4. Adams, R.D., Cawley, P., Pye, C.J., and Stone, B.J., ''A Vibration Technique for Non-Destructively Assessing the Integrity of Structures,'' *Journal of Mechanical Engineering Science* **20**(2): 93–100 (1978).
5. Gudmnundson, P., ''The Dynamic Behavior of Slender Structures with Cross Section Crack,'' *Journal of the Mechanics and Physics of Solids* **31**: 329–345 (1983).
6. Sinha, J.K., Friswell, M.I., and Edwards, S., ''Simplified Models for the Location of Crack in Beam Structures Using Measure Vibration Data,'' *Journal of Sound and Vibration* **251**(1): 13–38 (2002).
7. Liebowitz, H., Vanderveldt, H., and Harris, D.W., ''Carrying Capacity of Notched Column,'' *International Journal of Solids and Structures* **3**: 489–500 (1967).
8. Liebowitz, H., and Claus, W.D.S., Jr., ''Failure of Notched Columns,'' *Engineering Fracture Mechanics* **1**: 379–383 (1968).
9. Okamura, H., Liu, H.W., Chu, C.H., and Liebowitz, H., ''A Cracked Column under Compression,'' *Engineering Fracture Mechanics* **1**: 547–564 (1969).
10. Rizos, P.F., Aspragathos, N., and Dimarogonas, A.D., ''Identification of Crack Location and Magnitude in a Cantilever Beam from the Vibration Modes,'' *Journal of Sound and Vibration* **138**(3): 381–388 (1990).
11. Ostachowicz, W.M., and Krawczuk, C., ''Analysis of the Effect of Cracks on the Natural Frequencies of a Cantilever Beam,'' *Journal of Sound and Vibration* **150**(2): 191–201 (1991).
12. Bilello, C., *Theoretical and Experimental Investigation on Damaged Beams Under Moving Systems*. PhD Thesis, Universita' degli Studi di Palermo, Palermo, Italy (2001)
13. Krawczuk, M., Palacz, M., Ostachowicz, W., ''Genetic algorithm for fatigue crack detection in Timoshenko beam,'' *IUTAM Symposium on Evolutionary Methods in Mechanics*, Cracow, Poland, pp. 197–206 (2004).
14. Ong, Z.C., Rahman, A.G.A., and Ismail, Z., ''Determination of Damage Severity on Rotor Shaft Due To Crack Using Damage Index Derived from Experimental Modal Data,'' *Experimental Techniques* **38**: 18–30 (2014). DOI: 10.1111/j.1747-1567.2012.00823.x.
15. Chondros, T.J., Dimarogonas, A.D., and Yao, J., ''A Continuous Cracked Beam Vibration Theory,'' *Journal of Sound and Vibration* **215**(1): 17–34 (1998).
16. Ovanesova, A.V., and Suárez, L.E., ''Applications of Wavelet Transforms to Damage Detection in

Frame Structures,'' *Engineering Structures* **26**: 39–49 (2004).
17. El-Haddad, M.H., Ramadan, O.N., and Bazaraa, A.R., ''Analysis of Frames Containing Cracks and Resting on Elastic Foundations,'' *International Journal of Fracture* **45**: 81–102 (1990).
18. Caddemi, S., and Calió, I., ''The Exact Explicit Dynamic Stiffness Matrix of Multi-Cracked Euler–Bernoulli Beam and Applications to Damaged Frame Structures,'' *Journal of Sound and Vibration* **332**: 3049–3063 (2013).
19. Moghadam, A.A.A., Torabi, K., Moavenian, M., and Davoodi, R., ''Dynamic Modeling and Robust Control of an L-Shaped Microrobot Based on Fast Trilayer Polypyrrole-Bending Actuators,'' *Journal of Intelligent Material Systems and Structures* **24**: 484–498 (2013).
20. Grossi, R.O., *Variational Calculus, Theory and Applications, CIMNE*, Barcelona, Spain (2010).
21. Wolfram Research, Inc., Mathematica, Version 9.0, Champaign, Ilinois (2012)
22. Timoshenko, S.P., and Young, D.H., *Vibration Problems in Engineering, Van Nostrand Co., Inc.*, New York, NY (1955).
23. Lin, H.P., and Ro, J., ''Vibration Analysis of Planar Serial-Frame Structures,'' *Journal of Sound and Vibration* **262**: 1113–1131 (2003).
24. Albarracín, C.M., and Grossi, R.O., ''Vibrations of Elastically Restrained Frames,'' *Journal of Sound and Vibration* **285**: 467–476 (2005).
25. Rosales, M.B., Filipich, C.P., and Buezas, F.S., ''Crack Detection in Beam-Like Structures,'' *Engineering Structures* **31**: 2257–2264 (2009).
26. Labib, A., Dennedy, D., and Featherston, C., ''Free Vibration Analysis of Beams and Frames with Multiple Cracks for Damage Detection,'' *Journal of Sound and Vibration* **333**: 4991–5003 (2014).
27. Owolabi, G.M., Swamidas, A.S.J., and Seshadri, R., ''Crack Detection in Beams Using Changes in Frequencies and Amplitudes of Frequency Response Functions,'' *Journal of Sound and Vibration* **265**: 1–22 (2003).